Indian Journal of Engineering & Materials Sciences
Vol. 27, April 2020, pp. 418-423

Effect of surface mechanical attrition on microstructure and mechanical properties of hypoeuctectoid steel

Prashant Tadge* & Chandrabalan Sasikumar

Department of Materials Science & Metallurgical Engineering, Maulana Azad National Institute of Technology, Bhopal 462003, India

Received: 16 November 2017; Accepted: 28 January 2020

Effect of ultra-fine structure obtained by surface mechanical attrition treatment(SMAT) on microstructure, yield strength (YS), ultimate tensile strength (UTS) and microhardness of hypoeuctectoid steel have been studied in this paper. Surface alteration has been obtained by vibratory SMAT equipment with particular parameters for similar class of material. The SMAT has been carried out for different time periods such as 10, 20, 30 min. The pearlite and ferrite geometry present has been found intermixed after SMAT process. The microstructure shows a composite structure consisting of fiber/angular cementite particulates dispersed in a ferrite matrix. Thus, these structure obtained at 30 min of SMAT has significantly affected the mechanical properties. The SMAT affected layer has found to be 300µm which shows an increased Young's modulus from 140 GPa to 246 GPa. The yield stress (YS) and ultimate tensile strength (UTS) has been increased about 6% and 22% , respectively. The surface microhardness of the material has been changed from 226±5 $HV_{0.3}$ to 405±7 $HV_{0.3}$ by SMAT, which is attributed to the grain refinement and dispersion of fine carbide particles within the matrix.

Keywords: Surface mechanical attrition treatment, Microstructure, Composite layer, Mechanical properties

1 Introduction

The report of Gleiter on nano-crystalline material has initiated interest among various researches in developing advance materials with a combination of high strength, ductility and toughness. Atoms are made to produce bulked nanostructure metals and alloys. The first bulk nanostructure steel is produced by Bhadhesia at university of Cambridge. The team also produced a bainiticsteel by a special heat treatment technique[1, 2]. Garcia-Mateo et al had reported a technology for making nanostructure bainite in steel[3, 4]. Kimura et al had adopted mechanical milling technique to produced nanostructure steel[5]. Many research work are published on nano particulates strengthened metals and bulk nanostructure metallic materials are produced by ECAP, angular processing etc[6-10]. A considerable atoms are made in making nano-crystalline surface by SMAT. GuobinLi et al has produced a nano-crystalline surface with a mean size of 20nm crystals and reported a considerable decrement in friction coefficient and wear[11]. Lu and Lu is found to be the pioneer in this area and their group is identified the mechanism of grain refinement and the surface properties modified by SMAT[12, 13]. T. Balusamy et al has worked on pack boronizing of stainless steel by SMAT which increases the kinetics of boron diffusion[14]. In another interesting report Sahu et al has prepared room temperature carburizing by SMAT[15]. It is to be noted that many interesting studies were carried out to alter the pearlitic structure in steel samples to modify the steel properties. H. L. Yi has achieved a complete pearlitic structure in 0.4% carbon steel by controlled cooling rate[16]. It is possible to alter the interlamellar spacing and the cementite in ferrite matrix by SMAT. However, there are very few reports on the microstructural changes especially on ferrite and pearlite phases by SMAT. In the present work an attempt is made to produce anultra-fine composite structure consisting of fine carbides in ferrite matrix. The effect of these structural changes on the mechanical properties are investigated.

2 Experimental Procedures

A commercial grade medium carbon steel of 150x15x8 mm is used in the present investigation. The chemical composition of the steel is reported in Table 1. The samples were subjected to homogenization annealing at 800 °C prior to SMAT. An equipment operating at a vibrating frequency of 150Hz with hardened steel shots is used for SMAT. The SMAT was carried out for 10, 20, 30 min respectively. The experimental setup used for SMAT

*Corresponding author (E-mail: prashanttadge85@gmail.com)

process and procedure to carry out the work has been discussed in previous publication[17]. The treated samples were cut and prepared for investigating the microstructural analysis and mechanical properties. A JEOL 6390 scanning electron microscopy (SEM) is used for investigating the microstructural analysis.

X-ray diffraction (XRD) analysis was carried out in a Bruker AXE D2 PhaserAnalyserwith voltage of 40 kV using Cu-Kα radiation.A Universal Testing Machine (Mechatronic, India) is used to study the mechanical properties such as yield behavior, ultimate tensile strength, plastic deformation characteristics and toughness. AMicro-Vicker Hardness (MVH) Tester (HM-210/220B) supported with image graphing system is used for measuring the surface hardness before and after treatment.

3 Results and Discussion

3.1 Thickness of deformed region

Fig. 1 shows the typical cross-sectional image of 30 min SMATed samples. As shown the severe plastic deformed region depends upon the process time and found varying in the range of 300 to 350μm.

3.2 SEM analysis

The microstructure of the samples before and after SMAT is shown in Fig. 2 (a-d) respectively. The microstructure reveals the presence of ferrite and pearlite corresponding to 0.58% C steel i.e. the

Table 1 — Chemical composition of the steel (wt %).

C	Si	Mn	V	Ni	Cr	Cu	Fe
0.48	0.27	0.86	0.12	0.7	0.81	0.07	96.69

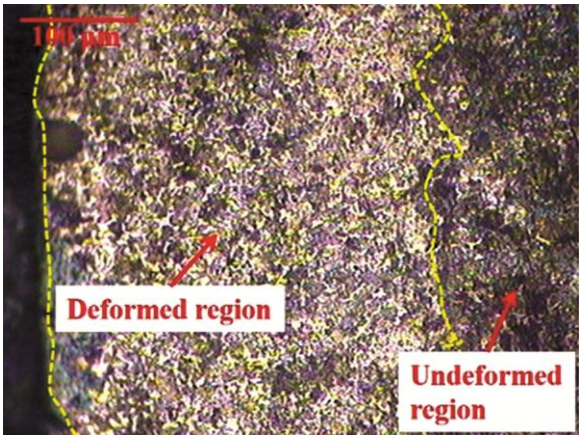

Fig. 1 — Microstructure of the cross-section of SMATed sample.

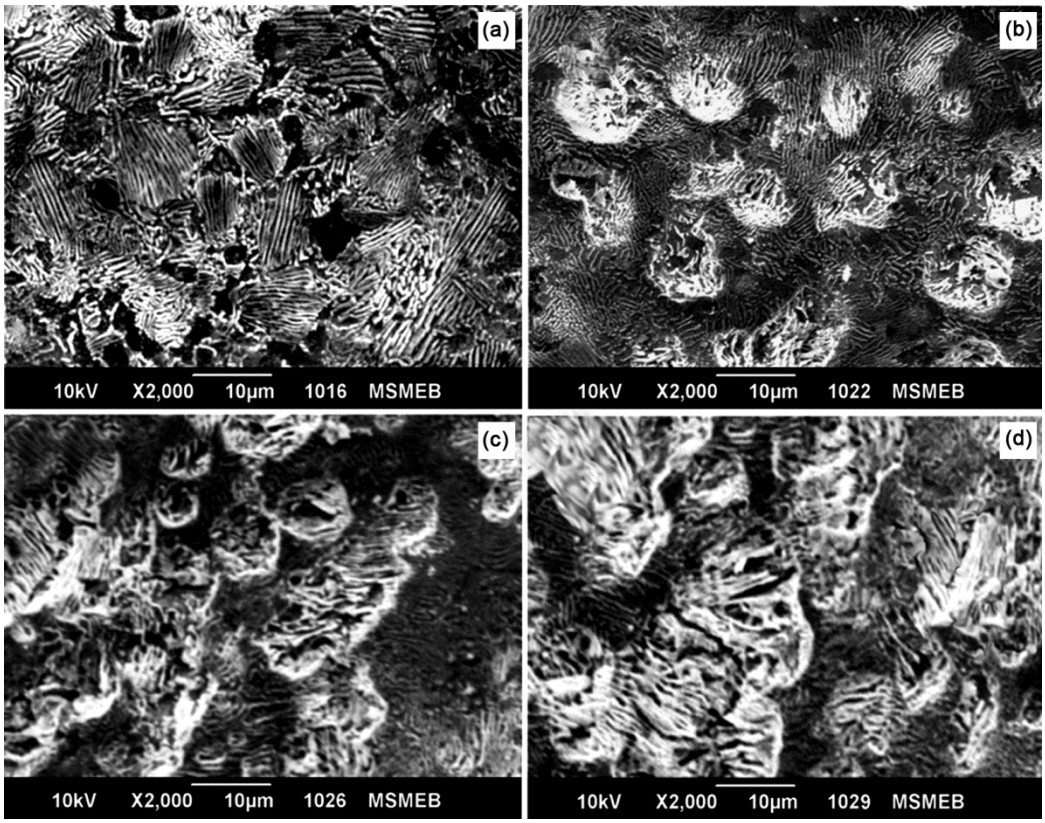

Fig. 2 — Microstructure of un-SMATed and SMATedsamples (a) 0 min, (b) 10 min, (c) 20 minand (d) 30 min.

pearlite content is about 70%. The cementite content found increasing by SMAT. It is noticed that the cementite content over the surface is about 80, 90 and 100% after 10, 20, and 30 min of SMAT respectively. The increment in cementite content is caused by intermixing of phases during SMAT. A similar observations are reported by Suryanarayana et al during mechanical alloying[18].

It is also found the grain size reduced considerably by SMAT. The variation of average grain diameter with SMAT time is plotted in Fig. 3.

The effect of SMAT on pearlitic phases were investigated in the present work. Fig. 4(a-d) shows the magnified SEM images of the samples with 0, 10, 20 and 30 min SMAT respectively. The result shows that the cementite platelets in a pearlitic phase is broken into finer size by SMAT. Cementite platelets of about 5 µm long is converted into fine fibers of 1µm dispersed randomly after 10 min of SMAT. On further processing the cementite fibers were broken into finer size particulates of 300 to 800 nm. In fact the overall surface structure transformed from cementite plates on pearlite matrix into fine carbide dispersed in ferrite matrix. Fig. 4(d) reveals that the cementite particulates mixed together and formed cementite lamellae in pearlite around proeutectoid ferrite. It is also observed that each cementite lamellae was obtained are connected with a thin layer and grown up in the same orientation. This cementite lamellae is a result from the rejection of carbon at the front of the

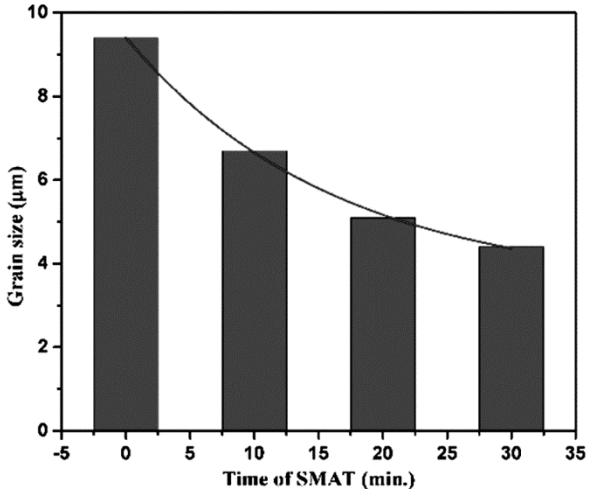

Fig. 3 — Grain size variation of treated surface with the duration of SMAT.

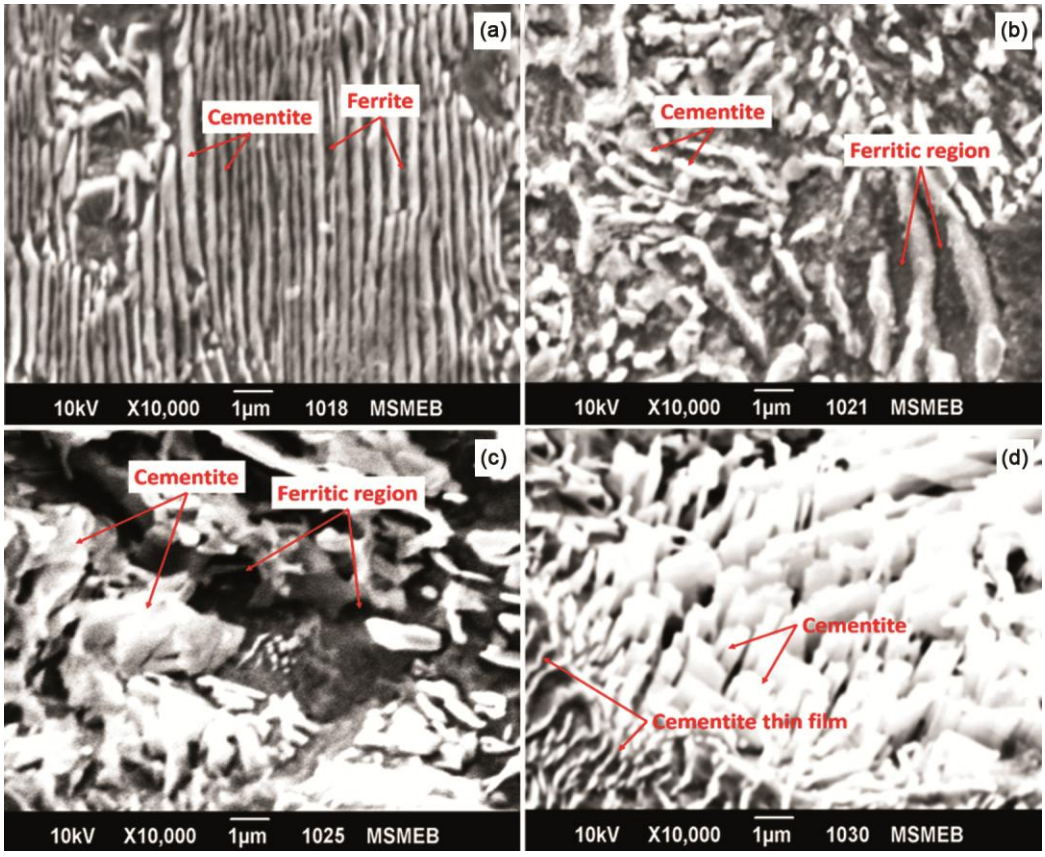

Fig. 4 — Magnified SEM images (a) without SMAT, (b) 10min SMAT, (c) 20 min SMAT and (d) 30 min SMAT samples.

growing proeuctectoid ferrite. Thus, the active participant of pearlite as the nucleus is cementite in hypoeuctectoid steel. The Zhang et al has proposed the similar morphology by heat treatment[19]. The particle size and percentage volume fraction of cementite found varying with process time and their details are reported in Fig. 5.

3.3 XRD pattern analysis

The XRD patterns of the samples before and after SMA treatments are shown in Fig. 6(a&b). It was observed from the obtained results that 30 min treated sample shows an evident broadening of the Bragg reflections as well as a shift in the centroid position of diffraction peaks comparative to the untreated sample. The shifting of peaks is attributed to the strain introduced by compressive residual stress as well as dissolution of carbon. The XRD results confirmed the presence of α-ferrite peaks (ICDD 00-006-0696) with reflections of (110) plane at 2θ (44.183°, 65.222°, 82.842°) and cementite peak (ICDD01-076-1877) with reflections of 103 plane at 2θ (44°).The intensity of peaks in the top bright surface layer of treated sample is higher than that in the untreated surface layer, which reveals that the volume fraction of cementite phase in the treated surface is possibly higher than that in the untreated surface.

3.4 Mechanical properties

The tensile stress–strain curves of carbon steel with SMAT are shown in Fig.7. The yield strength (YS), the ultimate tensile strength (UTS) and the change in percentage elongation (%E) determined by the curves plotted in Fig. 7. The percentage of cementite phase obtained by SMAT process also effect the ultimate tensile strength of material shown in Fig. 8. It is interesting to note that the composite structured steel has interesting combination of mechanical properties such as yield strength (YS) and ultimate tensile strength (UTS) increased from 647 MPa to 686 MPa & 757 MPa to 920 MPa with minor loss of ductility. The tensile curve also reveals that the yield strength slightly increases with the SMAT of 30 min. Thus, this also is in good agreement with the results stated by F.M. Al-Abbasi[20] and K.S. Kumar has reported the deformation mechanism of metals & alloys leads to reduce the grain size and improve the properties of materials[21]. This SMA treatment is one of the potential solution to achieve high strength with good toughness by producing fully cementite phase over the surface in medium carbon alloys with 0.48C wt%. Fig. 7 also shows the Young's modulus, which is significantly increased from 140 GPa to 246 GPa. The high modulus can be attributed to the compressive residual stress produced by SMAT. The modulus test was done by three-point bending test performed on Universal testing machine. The relationship between Young's modulus and stiffness can be written as

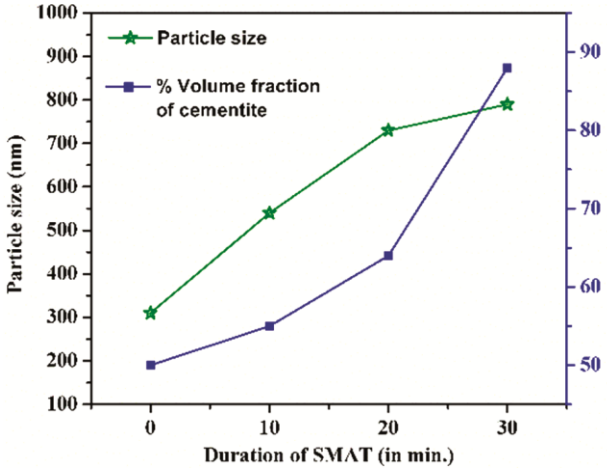

Fig. 5 — Variation of particle size and % volume fraction of cementite with duration of SMAT.

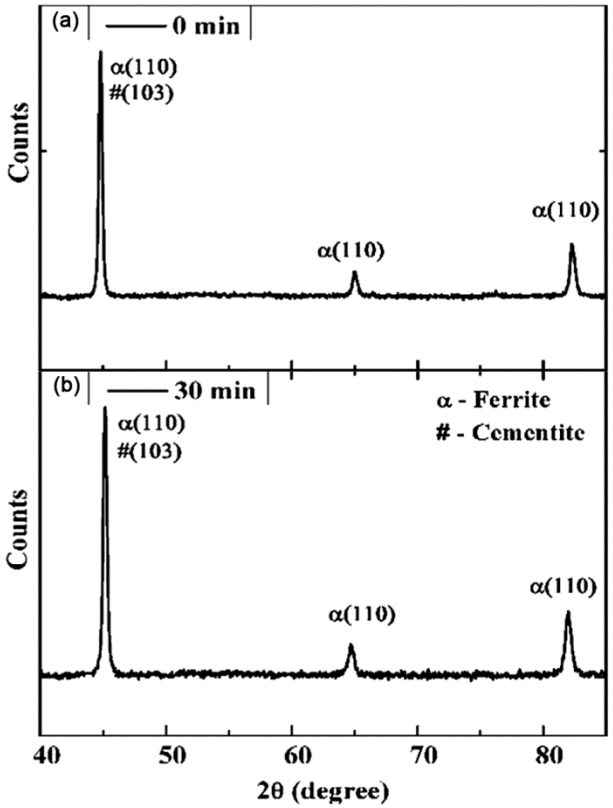

Fig. 6 — XRD patterns of specimens (a) 0 min SMAT and (b)30 min SMAT.

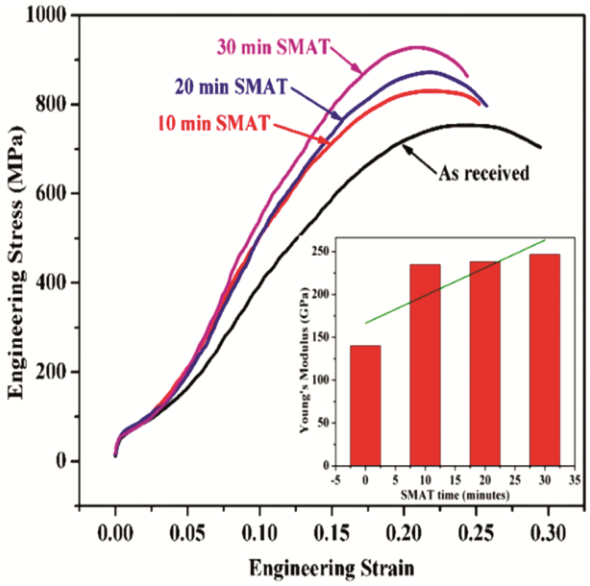

Fig. 7— Engineering stress-strain curves of SMATed and un-SMATed samples.

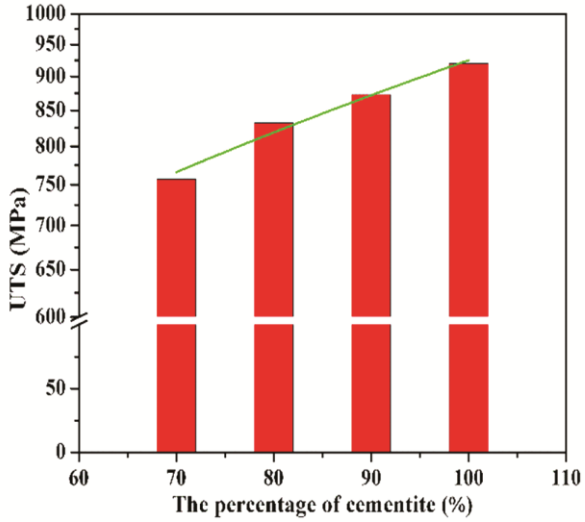

Fig. 8 — UTS variation with percentage of cementite within the surface.

$$E = \frac{kL^3}{48\,I} \quad \ldots (1)$$

Where, E is the Young's Modulus,
L is the span length,
k is the Stiffness ($k = {}^{F}/_{\delta}$)
F is the applied force,
δ is the deflection
and I is the inertia factor and can be written as

$$I = \frac{b\hbar^3}{12} \quad \ldots (2)$$

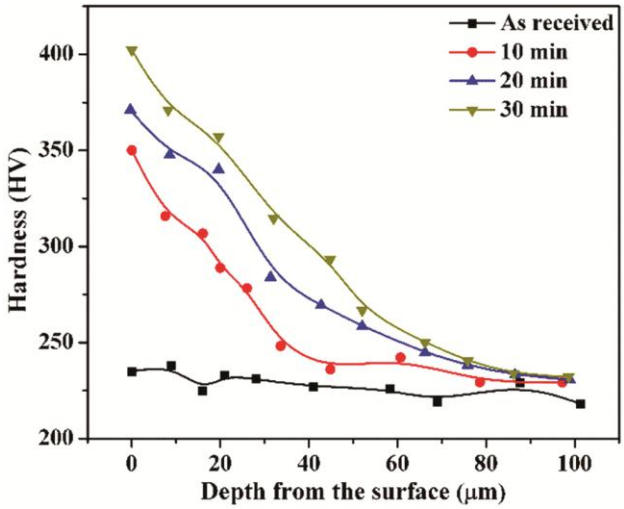

Fig. 9 — Micro-hardness variations along depth from the treated surface.

Where, b & h are the width and height of the material.

Fig. 9 shows the variation of micro-hardness along depth from the SMATed surface attains approximately 300μm. The high hardness value is due to the formation of ultra-fine structured layer of hard phase which is cementite. The hardness decreases gradually from the SMATed surface layer to the matrix. The hardness at the matrix was about 226±5 $HV_{0.3}$, however at the SMATed region the hardness was increased to about 405±7 $HV_{0.3}$. From the above it can be conclude that the hardness increases with treatment time and it is also reported by the different author's[22]. The surface hardness reached after 30 min is equivalent to hardened and tempered steel[17].

It is found that the cementite particulate over the surface is harder and stiffer than the matrix. These particles resist the movement of the matrix phase around the vicinity of each particle. Basically the particles bear the fraction of the load transferred by matrix leads to strengthening of material. The major portion of the applied load is enduring by matrix andthe dispersed particles hinder the motion of dislocation. These particles are thereby resisting the plastic deformation and improves the yield strength, ultimate tensile strength and hardness of material.

4 Conclusions

(i) The different morphologies of pearlite obtained by SMAT in a hypoeutectoid steel shows the growth of cementite phase which is attributed to the change in structure of cementite phase over the surface.

(ii) The microstructural and X-ray analysis confirms the presence of phases at the surface indicating the broadening of diffraction peaks after SMAT is accredited to reduction in crystallite size and increased in microstrain of lattice.

(iii) The effect of SMAT on the pearlitic phasealters the cementite lamellae which significantly enhance the mechanical properties of steel.

(iv) The SMAT produces anultra-fine composite structure consisting of fine carbides in the ferrite matrix thereby increasing the strength of steel.

(v) The strength properties were observed which depend on the SMAT processing time of the pearlitic structure. The tensile strength of treated sample was increased by 22% than untreated sample. And thenotable change of hardness was observed from 226 ± 5 $HV_{0.3}$to 405±7 $HV_{0.3}$ after SMAT, which is attributed to refined grain structure and dispersion of fine carbide particles within the matrix.

(vi) During SMAT on steel samples the active nucleus for pearlite is cementite which is developed from the thin cementite layers around the proeutectoid ferrite.

Acknowledgements

The authors wish to acknowledge the Director (MANIT Bhopal) for providing the facilities of equipment's and financial support. We also greatly appreciate the professors of MSME Department for supporting this research.

References

1 Bhadeshia H K D H, *Sci Technol Adv Mater*, 14 (2013) 014202.
2 Bhadeshia H K D H, *Nanostructured Bainite Proc R Soc A, London*, 466 (2010) 3.
3 Garcia-Mateo C, Caballero F & Bhadeshia H, *J Phys IV France*, 112 (2003) 285.
4 Yokota T, Mateo C G & Bhadeshia H, *Scr Mater*, 51 (2004) 767.
5 Kimura Y, Hidaka H & Takaki S, *Mat Trans JIM*, 40 (1999) 1149.
6 Isheim D, Gagliano M S, Fine M E & Seidman D N, *Acta Mater*, 54 (2006) 841.
7 Tsuji N, Saito Y, Utsunomiya H & Tanigawa S, *Scr Mater*, 40 (1999) 795.
8 Wang Y M, Ma E, Valiev R Z & Zhu Y T, *Adv Mater*, 16 (2004) 328.
9 Valiev R, Korznikov A & Mulyukov R, *Mater Sci Eng*, 59 (1997)234.
10 Semenova I P, Valiev R Z, Yakushina E B, Salimgareeva G H & Lowe T C, *J Mater Sci*, 43 (2008) 7354.
11 Guobin Li, Chen J & Guan D, *Trib Int J*, 43 (2010) 2216.
12 Lu K & Lu J, *Mater Sci Eng A*, 375 (2004) 38.
13 Zhu K Y, Vassel A, Brisset F, Lu K & Lu J, *Acta Mater*, 52 (2004) 4101.
14 Balusamy T, Narayanan T S N S, Ravichandran K, Park I S & Lee M H, *Surf Coat Technol*, 232 (2013) 60.
15 Sahu J N & Sasikumar C, *Trans Indian Inst Met*, 71 (2018) 915.
16 Yi H L, *Mater Sci Eng A*, 527 (2010) 7600.
17 Tadge P & Sasikumar C, *Trans Indian Inst Met*, 71 (2018) 1543.
18 Suryanarayana C & Al-Aqeeli N, *Prog Mater Sci*, 58 (2013) 383.
19 Zhang M X & Kelly P M, *Mater Charact*, 60 (2009) 545.
20 Al-Abbasi F, *Mater Sci and Eng A*, 527 (2010) 6904.
21 Kumar K, Swygenhoven H V & Suresh S, *Acta Mater*, 51 (2003) 5743.
22 Chamgordani S A, Miresmaeili R & Aliofkhazraei M, *Trib Int J*, 119 (2018) 744.